

Regular-to-Chaotic Tunneling Rates: From the Quantum to the Semiclassical Regime

Steffen Löck,¹ Arnd Bäcker,¹ Roland Ketzmerick,¹ and Peter Schlagheck^{2,3}

¹*Institut für Theoretische Physik, Technische Universität Dresden, 01062 Dresden, Germany*

²*Institut für Theoretische Physik, Universität Regensburg, 93053 Regensburg, Germany*

³*Division of Mathematical Physics, Lund Institute of Technology, PBox 118, 22100 Lund, Sweden*

(Dated: November 3, 2018)

We derive a prediction of dynamical tunneling rates from regular to chaotic phase-space regions combining the direct regular-to-chaotic tunneling mechanism in the quantum regime with an improved resonance-assisted tunneling theory in the semiclassical regime. We give a qualitative recipe for identifying the relevance of nonlinear resonances in a given \hbar -regime. For systems with one or multiple dominant resonances we find excellent agreement to numerics.

PACS numbers: 05.45.Mt, 03.65.Sq, 03.65.Xp

In mixed regular-chaotic systems the quantitative understanding of dynamical tunneling, which refers to classically forbidden transitions between phase-space regions that are separated by dynamical barriers [1], represents one of the most challenging open problems in semiclassical physics. In the early 1990s it was found [2–4] that tunneling rates between phase-space regions of regular motion are substantially enhanced by the presence of chaotic motion, which was termed chaos-assisted tunneling. Such dynamical tunneling processes are ubiquitous in molecular physics [1] and were realized with cold atoms in periodically modulated optical lattices [5, 6].

The fundamental process in this context is tunneling between states in a regular island and the surrounding chaotic region. In the quantum regime, $\hbar \lesssim \mathcal{A}$, where Planck's constant \hbar is smaller but comparable to the area of the regular island \mathcal{A} , this process is dominated by a *direct regular-to-chaotic tunneling* mechanism [7–9]. An approach to determine these direct tunneling rates was recently given in Ref. [10]. It relies on a fictitious integrable system that resembles the regular dynamics within the island under consideration, and has been applied to quantum maps [10], billiard systems [11], and the annular microcavity [12]. In the semiclassical regime, $\hbar \ll \mathcal{A}$, however, the direct tunneling contribution alone is incapable to describe the observed tunneling rates.

The existence of nonlinear resonances inside the regular island leads to peaks and plateaus in the tunneling rates. These can be qualitatively predicted by the theory of *resonance-assisted tunneling* [13, 14] as shown for quantum maps [14], periodically driven systems [15, 16], quantum accelerator modes [9], and for multidimensional molecular systems [17, 18]. Quantitatively, however, deviations of several orders of magnitude appear (see Fig. 1, gray line). Hence, both mechanisms alone give no reliable quantitative prediction of tunneling rates in generic systems.

In this Letter we derive a unified framework that combines the direct regular-to-chaotic and the resonance-assisted tunneling mechanisms. Beyond the direct tunneling contribution there are additional contributions: They consist of resonance-assisted tunneling steps within the regular island and, in contrast to previous studies

[9, 14], a final direct tunneling step to the chaotic sea; see insets in Fig. 1. This leads to an excellent prediction of tunneling rates from the quantum to the semiclassical regime. In particular, it includes the \hbar -regime, which is relevant for the search of experimental signatures of resonance-assisted tunneling.

Specifically, we consider one-dimensional kicked systems, described by the classical Hamiltonian $H(p, q, t) = T(p) + V(q) \sum_{k \in \mathbb{Z}} \delta(t - k)$ and by the quantum time-evolution operator $U = \exp[-iV(q)/\hbar] \exp[-iT(p)/\hbar]$, which exhibit one major regular island embedded in the chaotic sea. This mixed phase-space structure gives rise to eigenstates of U that are mainly regular or chaotic, i.e. concentrated on a torus inside the regular region or spread out over the chaotic sea. However, they do have

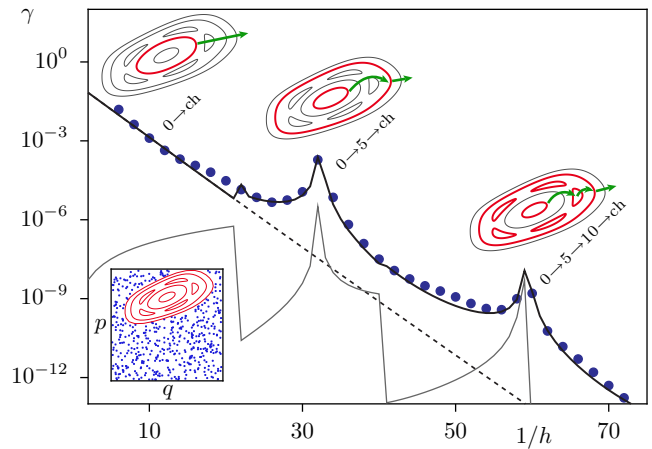


FIG. 1: (Color online) Dynamical tunneling rates γ from the innermost quantized torus ($m = 0$) of a regular island with one dominant 5:1 resonance. Numerical data (dots) is compared to the prediction of Eq. (1) (solid line) and previous results in the quantum regime due to the direct tunneling process (dashed line, Eq. (2), Ref. [10]) and in the semiclassical regime due to resonance-assisted tunneling (gray solid line, Ref. [14]). The lower inset shows the phase space of the system [19]. The upper insets illustrate the dominant tunneling steps for three values of \hbar .

small components in the other region of phase space. Consequently, a wave packet started on the m th quantized torus ($m = 0, 1, \dots, m_{\max} - 1$) of the island will, in the presence of absorbing boundary conditions in the chaotic sea, leak out from the island $\sim e^{-\gamma_m t}$ with a characteristic tunneling rate γ_m . It describes the mean coupling to the chaotic sea, where fluctuations from individual chaotic states are averaged.

We now consider the presence of a prominent nonlinear $r:s$ resonance (s oscillations match r driving periods) within the island. For small \hbar , this resonance gives rise to couplings between different regular states [13], which compete with direct tunneling and lead to additional pathways into the chaotic sea. We derive (see below) the tunneling rate of the m th quantized state as

$$\gamma_m = \gamma_m^d + |A_{m,r}^{(r:s)}|^2 \gamma_{m+r}^d + |A_{m,r}^{(r:s)} A_{m,2r}^{(r:s)}|^2 \gamma_{m+2r}^d + \dots \quad (1)$$

The first term describes the direct tunneling process from the m th quantized torus to the chaotic sea with the rate γ_m^d , neglecting any influence from nonlinear resonances. In the second term the coefficient $A_{m,r}^{(r:s)}$ describes one resonance-assisted tunneling step from the m th to the $(m+r)$ th quantized torus via an $r:s$ resonance, while the factor γ_{m+r}^d describes the subsequent direct tunneling into the chaotic sea. The last term accounts for two resonance-assisted and one direct tunneling step. The three terms are visualized as insets in Fig. 1 in the h -regime where they are most relevant. Note, that the final step to the chaotic sea occurs due to direct tunneling, which is in contrast to previous studies [9, 14], where another resonance-assisted step is used. We now discuss (i) the direct tunneling rates γ_m^d , (ii) the coefficients $A_{m,r}^{(r:s)}$, and (iii) the derivation of Eq. (1).

(i) The direct tunneling rates can be predicted by an approach [10] using a fictitious integrable system which has to be chosen such that its classical dynamics resembles the dynamics of the mixed system within the regular island as closely as possible. The eigenstates $|m\rangle_0$ of the fictitious integrable Hamiltonian H_0 are localized in the regular region of H and decay outside. Using Fermi's golden rule, $\gamma_m^d \equiv \sum_{\text{ch}} |v_{|m\rangle_0, \text{ch}}|^2$, in which $v_{|m\rangle_0, \text{ch}} = \langle \psi_{\text{ch}} | U | m \rangle_0$ couples $|m\rangle_0$ to different chaotic states, the direct tunneling rates are given as [10]

$$\gamma_m^d = \|P_{\text{ch}}(U - U_{\text{reg}})|m\rangle_0\|^2 \quad (2)$$

where $U_{\text{reg}} \equiv \exp(-iH_0/\hbar)$ and P_{ch} is a projector onto the chaotic region. Here we assume that there are no additional phase-space structures within the chaotic sea that affect the direct tunneling rates. Note, that this approach is applicable for general systems with a mixed phase space [11, 12]. Different methods for the determination of the fictitious integrable system can be employed, based on the Lie transformation [21] (used in Figs. 1 and 2) or on the frequency map analysis [22] (used in Fig. 3). Details will be presented elsewhere [20].

(ii) The coefficients $A_{m,kr}^{(r:s)}$ in Eq. (1) depend on nonlinear resonances. The classical dynamics of such an $r:s$

resonance is described in the corotating frame by the effective pendulum Hamiltonian [13, 21]

$$H_{\text{res}}(I, \theta) = H_0(I) - \Omega_{r:s}(I - I_{r:s}) + 2\mathcal{V}_r(I) \cos(r\theta) \quad (3)$$

with $\Omega_{r:s} = 2\pi s/r$, where $2\mathcal{V}_r(I) \cos(r\theta)$ is the perturbation in terms of the local action-angle variables (I, θ) . The simplest approach is the direct quantization of Eq. (3) in action-angle space by neglecting the action dependence of the coupling using $\mathcal{V}_{r:s} \equiv \mathcal{V}_r(I_{r:s})$ and by making a quadratic approximation of $H_0(I)$ around the action $I_{r:s}$ of the $r:s$ resonance, leading to $H_0(I) - \Omega_{r:s}(I - I_{r:s}) \approx (I - I_{r:s})^2/2m_{r:s}$. It is then found that the $r:s$ resonance couples the m th excited state $|m\rangle_0$ of the resonance-free island to the state $|m+r\rangle_0$ with the coefficient

$$A_{m,kr}^{(r:s)} = \frac{\mathcal{V}_{r:s} e^{i\varphi}}{E_m - E_{m+kr} + kr\hbar\Omega_{r:s}} \quad (4)$$

where $E_m = [I_m - I_{r:s}]^2/(2m_{r:s}) + \Omega_{r:s}I_m$ with $I_m \equiv \hbar(m + 1/2)$ are the eigenvalues of the approximation of H_0 . $I_{r:s}$, $\mathcal{V}_{r:s}$, and $m_{r:s}$ can be extracted from the classical phase space [14, 23].

(iii) To derive Eq. (1) we start from Eq. (3) and apply quantum perturbation theory to obtain the perturbed regular states

$$|m\rangle = |m\rangle_0 + A_{m,r}^{(r:s)} |m+r\rangle_0 + A_{m,r}^{(r:s)} A_{m,2r}^{(r:s)} |m+2r\rangle_0 + \dots \quad (5)$$

These are now inserted into Fermi's golden rule $\gamma_m \equiv \sum_{\text{ch}} |v_{|m\rangle, \text{ch}}|^2$ with $v_{|m\rangle, \text{ch}} = \langle \psi_{\text{ch}} | U | m \rangle$. Using the definition of γ_m^d and neglecting "off-diagonal" contributions of mixed terms (which at most amount to corrections of the order of a factor two) leads to Eq. (1).

In the following we discuss two important improvements to the coefficients $A_{m,kr}^{(r:s)}$ in (ii): (iia) On one hand, the quadratic approximation of $H_0(I)$ around $I = I_{r:s}$ fails to predict the correct unperturbed energies E_m especially for resonances close to the border of the regular island such that the peaks in the tunneling rates are located at a wrong position (see Figs. 2 and 3, dotted lines). Here, we use a semiclassical procedure to determine a *global* approximation of the unperturbed system $H_0(I)$ [10]. Using its eigenenergies \bar{E}_m in Eq. (4) leads to improved peak positions in the tunneling rates.

(iib) On the other hand, the action dependence of the perturbation $\mathcal{V}_r(I)$ needs to be properly accounted for. Here we use the fact that the Hamiltonian $H(p, q, t)$ is analytic in the "harmonic oscillator" variables $(P, Q) \equiv \sqrt{2I}(-\sin\theta, \cos\theta)$ which result from (p, q) through an analytical canonical transformation. This yields $\mathcal{V}_r(I) \propto I^{\frac{r}{2}}$ in lowest order in I and $\mathcal{V}_r(I) e^{\pm ir\theta} \propto (Q \pm iP)^r$. Quantization in Q -space then amounts to replacing $(Q \pm iP)/\sqrt{2\hbar}$ by the ladder operator \hat{a} satisfying $\hat{a}|m\rangle_0 = \sqrt{m}|m-1\rangle_0$. We therefore obtain in leading order

$$\bar{\mathcal{V}}_{r:s}^{m,kr} \equiv {}_0\langle m' | H_{\text{res}} | m' + r \rangle_0 = \mathcal{V}_{r:s} \left(\frac{\hbar}{I_{r:s}} \right)^{\frac{r}{2}} \sqrt{\frac{(m' + r)!}{m'!}} \quad (6)$$

with $m' = m + (k - 1)r$. These new coupling parameters $\bar{V}_{r:s}^{m,kr}$ depend on \hbar and on the quantum number m of the coupled regular state. They replace $\mathcal{V}_{r:s}$ in Eq. (4) and improve the tunneling rates in between the peaks.

We now predict dynamical tunneling rates with Eq. (1) using (i) the direct tunneling rates γ_m^d from Eq. (2) describing the decay of the regular states by ignoring the influence of resonances, (ii) the improved eigenenergies \bar{E}_m of $H_0(I)$ and (iib) the action dependent couplings $\bar{V}_{r:s}^{m,kr}$ from Eq. (6). Fig. 1 shows a comparison between this theoretical prediction (solid line) and numerical data (dots), obtained using absorbing boundary conditions in the chaotic sea. In contrast to the sole application of direct tunneling with Eq. (2) (dashed line) or resonance-assisted tunneling according to Ref. [14] (gray line) we find excellent agreement from the quantum to the semiclassical regime. The phase space of the system is depicted in the inset of Fig. 1. It shows one dominant 5:1 resonance inside the regular island. All other resonances are small and do not contribute to the tunneling rates for the shown values of \hbar . We find that the direct tunneling rates γ^d following from Eq. (2) explain the numerical data for $1/\hbar \lesssim 20$. For larger $1/\hbar$ the 5:1 resonance is important and gives rise to two characteristic peaks corresponding to the coupling of the ground state $m = 0$ to $m = 5$ and $m = 10$. Our theoretical prediction excellently reproduces the peak positions and heights.

As a next example we consider a situation where three dominant resonances exist, namely a 5:1 resonance near the center of the regular island, an 11:2, and an outer 6:1 resonance, see the inset in Fig. 2. Here, multi-resonance couplings occur and the tunneling rates from the

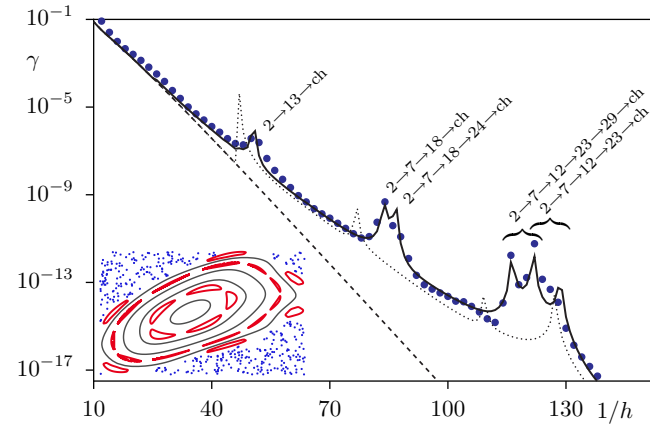


FIG. 2: (Color online) Dynamical tunneling rates γ from the quantized torus $m = 2$ of a regular island with three dominant resonances. Numerical data (dots) is compared to the prediction of Eq. (1) (solid line). For comparison the direct tunneling contribution (dashed line, Eq. (2), Ref. [10]) and the result of Eq. (1) without the improvements (iia) and (iib) is presented (dotted line). The inset shows the regular island of the system [19] and the dominant 5:1, 11:2, and 6:1 resonances which cause tunneling steps as indicated by labels.

torus $m = 2$ are determined with Eq. (1) by a summation over all relevant $r:s$ resonances. For example the peak at $1/\hbar \approx 84$ in the tunneling rates is caused by the coupling of the state $m = 2$ to the 18th excited state via the 5:1 and the 11:2 resonance. In Fig. 2 we compare numerical data (dots) to the prediction of Eq. (1) and find very good agreement. For comparison we also show the rates (dotted line) that result from using Eq. (1) together with Eq. (4) without the improvements (iia) and (iib). We still find overall agreement to the average decrease of the tunneling rates with $1/\hbar$. However, the reproduction of the positions and heights of the individual peaks requires to use a global approximation for the unperturbed energies (iia) and to take into account the action dependence of the coupling matrix elements (iib).

The paradigmatic model of quantum chaos is the standard map $[T(p) = p^2/2, V(q) = -K/(4\pi^2) \cos(2\pi q)]$. For $K = 3.5$ it has a large generic regular island with a dominant 6:2 resonance and further relevant 14:5 and 8:3 resonances. These are the largest low-order resonances. Fig. 3 shows the comparison between numerical data and the prediction of Eq. (1) far into the semiclassical limit. We find quantitative agreement over 30 orders of magnitude in γ . The direct tunneling process is relevant for $1/\hbar \lesssim 30$ beyond which several regimes for the tunneling rates caused by different resonances are identified. We attribute the small deviations below the prediction of Eq. (1) to destructive interference of different tunneling sequences leading to the same final state.

An important question is when the resonances become relevant, i.e. where is the transition between the direct tunneling regime $\hbar \lesssim \mathcal{A}$, where resonances play no role,

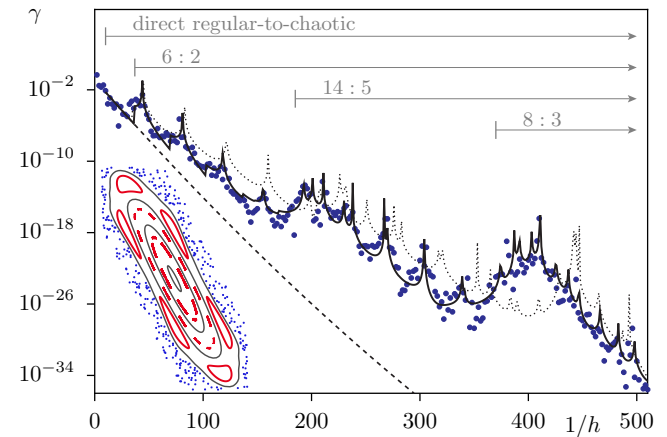


FIG. 3: (Color online) Dynamical tunneling rates γ from the innermost quantized torus $m = 0$ of the regular island for the standard map at $K = 3.5$. Numerical data (dots) is compared to the prediction of Eq. (1) (solid line). For comparison the direct tunneling contribution (dashed line, Eq. (2), Ref. [10]) and the result of Eq. (1) without the improvements (iia) and (iib) is presented (dotted line). The inset shows the island with the dominant 6:2, 14:5, and 8:3 resonances and the arrows indicate the regimes where they start to become relevant.

and the resonance-assisted tunneling regime $h \ll \mathcal{A}$. The latter requires that the $(m+r)$ th quantized torus exists inside the island, i.e.

$$\frac{\mathcal{A}}{h} \geq m + r + \frac{1}{2}. \quad (7)$$

The position h_{peak} of the first peak in γ_m arises when Eq. (4) diverges for $E_m - E_{m+r} + r\hbar\Omega_{r:s} = 0$. Using the quadratic approximation for $H_0(I)$, we find

$$\frac{\mathcal{A}_{r:s}}{h_{\text{peak}}} = m + \frac{r}{2} + \frac{1}{2} \quad (8)$$

with $\mathcal{A}_{r:s} \equiv 2\pi I_{r:s}$. The first peak appears when the $r:s$ resonance encloses $m+r/2$ quantized tori. However, the influence of the resonance may appear much earlier than $1/h_{\text{peak}}$. We define the transition point $1/h_{\text{res}}$ when the first two terms in Eq. (1) are equal. Using $\sqrt{2m_{r:s}}\mathcal{V}_{r:s} = \Delta\mathcal{A}_{r:s}/16$ [14], where $\Delta\mathcal{A}_{r:s}$ is the area enclosed between the separatrices of the $r:s$ resonance, we obtain

$$\frac{\Delta\mathcal{A}_{r:s}}{rh_{\text{res}}} \frac{\Delta\mathcal{A}_{r:s}}{\mathcal{A}_{r:s}} \sqrt{\frac{\gamma_{m+r}^d(h_{\text{res}})}{\gamma_m^d(h_{\text{res}})}} \frac{1}{(h_{\text{res}}/h_{\text{peak}} - 1)} = \frac{128}{\pi^2}. \quad (9)$$

This criterion explicitly involves the size $\Delta\mathcal{A}_{r:s}$ of the $r:s$ resonance chain measured with respect to r Planck cells and to the area $\mathcal{A}_{r:s}$ enclosed by the resonance, as well as the ratio of the direct tunneling rates from the $(m+r)$ th and the m th quantized torus. As the left-hand side of Eq. (9) is expected to display a monotonous

increase with $1/h_{\text{res}}$ towards the singularity at $1/h_{\text{peak}}$, resonance chains with a large area $\Delta\mathcal{A}_{r:s}$ will lead to a lower transition point $1/h_{\text{res}}$ at which the crossover from direct to resonance-assisted tunneling appears. While, e.g., the first peak of the 5:1 resonance in Fig. 2 appears at $1/h_{\text{peak}} \approx 130$ it dominates the tunneling process already at $1/h_{\text{res}} \approx 40$ which is even before the contributions from other resonances set in. Equations (8) and (9) confirm the intuition that low-order resonances with small r,s and large $\Delta\mathcal{A}_{r:s}$ are most relevant.

In conclusion, we have combined an improved resonance-assisted tunneling theory with the theory of direct tunneling using a fictitious integrable system to predict dynamical tunneling rates from the quantum regime, $h \lesssim \mathcal{A}$, to the semiclassical regime, $h \ll \mathcal{A}$. Excellent quantitative agreement with numerically determined tunneling rates is found on the level of individual resonance peaks, which emphasizes the validity of the underlying direct and resonance-assisted mechanisms. We therefore expect that these mechanisms leave their characteristic traces in semiclassical approaches based on complex classical trajectories [24], and allow one to understand and predict tunneling rates also in more complex, multidimensional quantum systems.

We thank S. Keshavamurthy for useful discussions and the DFG for support within the Forschergruppe 760 ‘‘Scattering Systems with Complex Dynamics’’.

-
- [1] M. J. Davis and E. J. Heller, *J. Chem. Phys.* **75**, 246 (1981).
- [2] W. A. Lin and L. E. Ballentine, *Phys. Rev. Lett.* **65**, 2927 (1990).
- [3] O. Bohigas, S. Tomsovic, and D. Ullmo, *Phys. Rep.* **223**, 43 (1993).
- [4] S. Tomsovic and D. Ullmo, *Phys. Rev. E* **50**, 145 (1994).
- [5] D. A. Steck, W. H. Oskay, and M. G. Raizen, *Science* **293**, 274 (2001).
- [6] W. K. Hensinger *et al.*, *Nature* **412**, 52 (2001).
- [7] J. D. Hanson, E. Ott, and T. M. Antonsen, *Phys. Rev. A*, **29**, 819 (1984).
- [8] V. A. Podolskiy and E. E. Narimanov, *Phys. Rev. Lett.* **91**, 263601 (2003); see Ref. [25] for a corrected formula.
- [9] M. Sheinman, S. Fishman, I. Guarneri, and L. Rebuzzini, *Phys. Rev. A* **73**, 052110 (2006).
- [10] A. Bäcker, R. Ketzmerick, S. Löck, and L. Schilling, *Phys. Rev. Lett.* **100**, 104101 (2008).
- [11] A. Bäcker, R. Ketzmerick, S. Löck, M. Robnik, G. Vidmar, R. Höhmann, U. Kuhl, and H.-J. Stöckmann, *Phys. Rev. Lett.* **100**, 174103 (2008).
- [12] A. Bäcker, R. Ketzmerick, S. Löck, J. Wiersig, and M. Hentschel, *Phys. Rev. A* **79**, 063804 (2009).
- [13] O. Brodier, P. Schlagheck, and D. Ullmo, *Phys. Rev. Lett.* **87**, 064101 (2001); *Ann. of Phys.* **300**, 88 (2002).
- [14] C. Eltschka and P. Schlagheck, *Phys. Rev. Lett.* **94**, 014101 (2005).
- [15] A. Mouchet, C. Eltschka, and P. Schlagheck, *Phys. Rev. E* **74**, 026211 (2006).
- [16] S. Wimberger, P. Schlagheck, C. Eltschka, and A. Buchleitner, *Phys. Rev. Lett.* **97**, 043001 (2006).
- [17] S. Keshavamurthy, *J. Chem. Phys.* **122**, 114109 (2005).
- [18] S. Keshavamurthy, *Phys. Rev. E* **72**, 045203(R) (2005).
- [19] Similarly to Ref. [10] we start with functions $t'(p) = 1/2 \pm (1-2p)$ for $0 < \pm p < 1/2$ and $v'(q) = -rq + Rq^2 + Zq^3$ for $-1/2 < q < 1/2$. Smoothing the periodically extended functions with a Gaussian, $G(z) = \exp(-z^2/2\varepsilon^2)/\sqrt{2\pi\varepsilon^2}$, gives analytic functions $T'(p) = \int dz t'(p+z)G(z)$ and $V'(q) = \int dz v'(q+z)G(z)$. We take $r = 0.74$, $R = 0.2$, $Z = 1$, $\varepsilon = 0.002$ in Fig. 1 and $r = 0.72$, $R = 0.45$, $Z = 1.2$, $\varepsilon = 0.002$ in Fig. 2.
- [20] A. Bäcker, R. Ketzmerick, S. Löck, in preparation.
- [21] A. J. Lichtenberg and M. A. Leibermann, *Regular and Stochastic Motion* (Springer, New York, 1983).
- [22] J. Laskar, C. Froeschlé, and A. Celletti, *Physica D* **56**, 253 (1992).
- [23] S. Tomsovic, M. Grinberg, and D. Ullmo, *Phys. Rev. Lett.* **75**, 4346 (1995).
- [24] A. Shudo and K. S. Ikeda, *Phys. Rev. Lett.* **74**, 682 (1995); *Physica D* **115**, 234 (1998).
- [25] M. Sheinman, Masters thesis, Technion, 2005, Eq. (A.14).